Roles of Barotropic Instability across the Moat in Inner Eyewall Decay and Outer Eyewall Intensification: Essential Dynamics

TSZ-KIN LAI,[a] ERIC A. HENDRICKS,[b] M. K. YAU,[a] AND KONSTANTINOS MENELAOU[c]

[a] *Department of Atmospheric and Oceanic Sciences, McGill University, Montreal, Quebec, Canada*
[b] *National Center for Atmospheric Research, Boulder, Colorado*
[c] *Environment and Climate Change Canada, Dorval, Quebec, Canada*

(Manuscript received 3 June 2020, in final form 1 February 2021)

Introduction

- The mechanisms of inner eyewall decay and outer eyewall intensification:
  - The upper-level outflow of inner eyewall is opposed by the forced inflow from outer eyewall. The forced flow descent and the N^2 increased inside the outer eyewall.
  - Cutoff effect. The outer eyewall act as a barrier to intercept the low-level inflow. The supply of AAM and moisture is reduced so that the inner eyewall wind speeds and convection cannot maintain.
- Two mechanisms may work together: the descent from the outer eyewall of Hurricane Gonzalo (2014) overrode the updraft of the weakening inner eyewall in the downshear quadrants. (Didlake et al. 2017)
- TCs may weaken due to the cool and dry boundary layer air with low θ_e transported by the primary rainband convective downdraft. Strong low θ_e transports to the inner eyewall when the two eyewalls are close, and the inner eyewall dissipates.
  (Powell 1990; Zhou and Wang 2011)

Introduction

- Barotropic instability (BI) exists when the radial vorticity gradient changes sign within the domain of interest and can result in asymmetric development of vorticity, such as polygonal eyewalls and potential vorticity mixing. (Schubert et al. 1999)

- The vorticity generated by the diabatic heating in eyewall and dissipated by the friction in eye causes the annular vorticity structure and BI. (Rozoff et al. 2009)

- BI is the source of asymmetry of the existence of a WN2 VRW in the elliptical eyewall of Hurricane Olivia (1994). (Reasor et al. 2000)

- The vertical swirls resulted from the vorticity mixing between the eye and eyewall due to the BI in a 2D barotropic model are similar to the cloud pattern of the eye of TCs, such as Hurricane Isabel (2003). (Kossin et al. 2002; Kossin and Schubert 2004)

Introduction

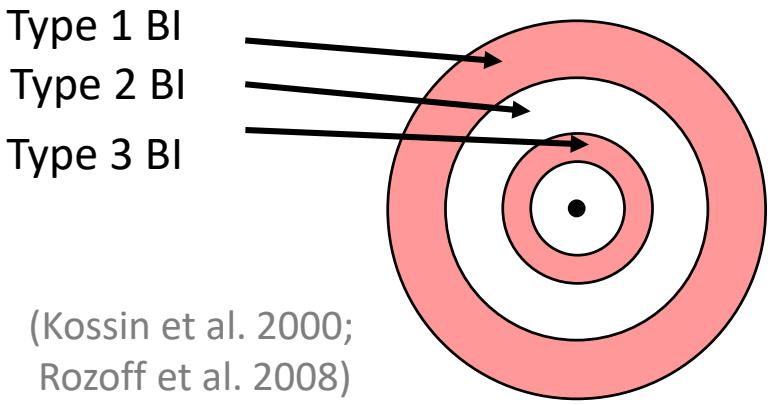

(Kossin et al. 2000; Rozoff et al. 2008)

- After the onset of the type-2 BI, the low-level inner core circulation of the simulated Hurricane Wilma (2005) had a period of rapid decay, coinciding with the emergence of a WN2 radial flow, which decayed the inner eyewall. (Lai et al. 2019)
- The AAM over the lower and middle levels in the inner eyewall decreased as a result of the net radially outward transport of AAM by the **negative eddy radial transport of eddy AAM** caused by the type-2 BI. (Lai et al. 2021)
- The eddy processes is nonnegligible and resulted from **the deviation from 45º** phase difference between the **radial gradient of eddy AAM** and **eddy radial flow**. Type-2 BI with the most unstable mode has a WN2 structure.
- The study: Explore the reason of the eddy processes by shallow water model, AAM budget analysis, and balanced wave dynamics.

Methodology

2D nonlinear shallow water model

B.C.: Double open BC with sponge layer
Time integrating scheme: Leapfrog with Robert–Asselin filter

$$\frac{\partial u}{\partial t} + u\frac{\partial u}{\partial x} + v\frac{\partial u}{\partial y} - f_0 v = -g\frac{\partial h}{\partial x} - \nu\nabla^4 u,$$

$$\frac{\partial v}{\partial t} + u\frac{\partial v}{\partial x} + v\frac{\partial v}{\partial y} + f_0 u = -g\frac{\partial h}{\partial y} - \nu\nabla^4 v,$$

$$\frac{\partial h}{\partial t} + \frac{\partial (uh)}{\partial x} + \frac{\partial (vh)}{\partial y} = 0,$$

$f_0 = 4.615 \times 10^{-5}\ 1/s$
$(18.5°N)$

Methodology

2D linear shallow water model
(linearized about an axisymmetric vortex in gradient wind balance)

B.C.: Double open BC with sponge layer
Time integrating scheme: Leapfrog with Robert–Asselin filter

$$u = u_0 + u^*$$
$$v = v_0 + v^*$$
$$h = h_0 + h^*$$

h_0: gradient wind balance

$f_0 = 4.615 \times 10^{-5}\ 1/s$
$(18.5°N)$

$$\frac{\partial u^*}{\partial t} + u_0\frac{\partial u}{\partial x} + u^*\frac{\partial u_0}{\partial x} + v_0\frac{\partial u}{\partial y} + v^*\frac{\partial u_0}{\partial y} - f_0 v = -g\frac{\partial h}{\partial x} - \nu\nabla^4 u,$$

$$\frac{\partial v^*}{\partial t} + u_0\frac{\partial v}{\partial x} + u^*\frac{\partial v_0}{\partial x} + v_0\frac{\partial v}{\partial y} + v^*\frac{\partial v_0}{\partial y} + f_0 u = -g\frac{\partial h}{\partial y} - \nu\nabla^4 v,$$

$$\frac{\partial h^*}{\partial t} + \frac{\partial(u_0 h + u^* h_0)}{\partial x} + \frac{\partial(v_0 h + v^* h_0)}{\partial y} = 0.$$

Methodology

- Experiment design:
  - z from 0.5 to 3.5 km with interval 0.5 km
  - dx = dy = 1 km, 664*664 grid points
  - Conduct nonlinear and linear SWM for 12 hr

Lai et al., 2021

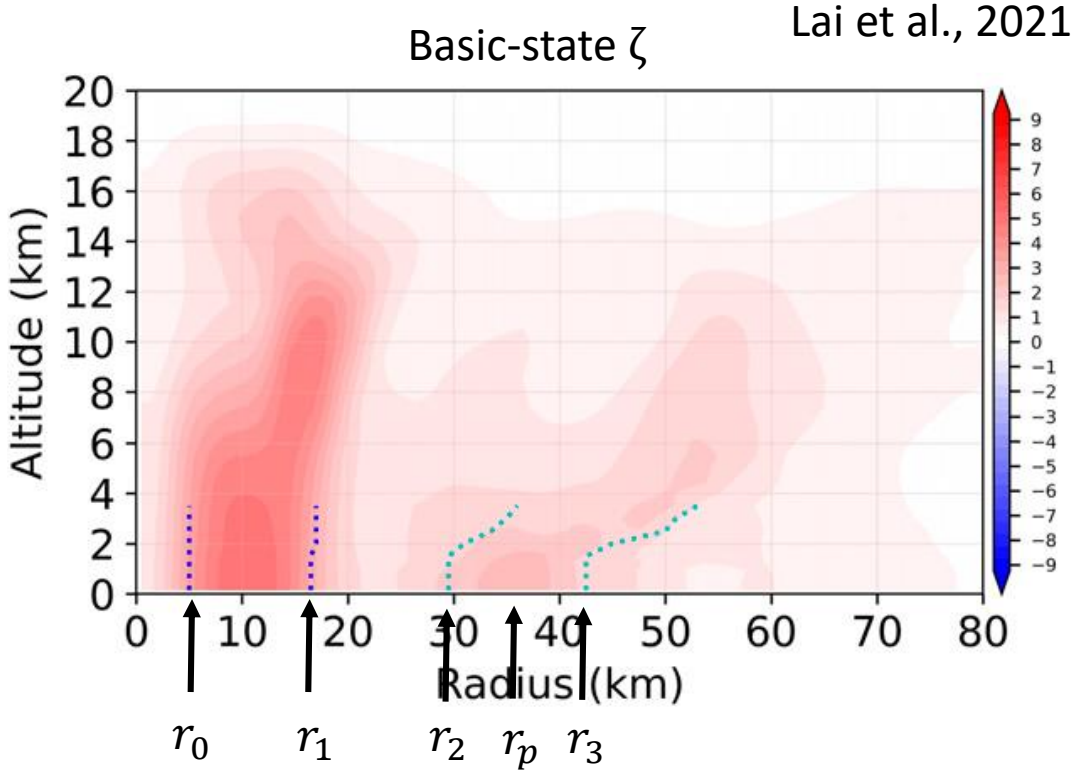

Perturb the vorticity in the moat by the equation:

$$\zeta'(r,\lambda) = \zeta_{\text{amp}} \sum_{m=1}^{12} \cos(m\lambda) \begin{cases} 0, & 0 \le r \le r_1 - d \\ S[(r_1 + d - r)/2d], & r_1 - d \le r \le r_1 + d \\ 1, & r_1 + d \le r \le r_2 - d \\ S[(r - r_2 + d)/2d], & r_2 - d \le r \le r_2 + d \\ 0, & r \ge r_2 + d, \end{cases}$$

ζ_{amp}: 0.01% minimum vorticity in the moat

Altitude (km)	r_0	r_1	r_2	r_p	κ	r_3
≤1.5	5.0	16.5	29.5	36.0	6.5	42.5
2.0	5.0	17.0	31.0	38.0	7.0	45.0
2.5	5.0	17.0	33.5	43.0	7.0	50.0
3.0	5.0	17.0	35.0	46.0	5.0	51.0
3.5	5.0	17.0	36.0	48.0	5.0	53.0

Overview of the shallow water experiments

Colored: ζ
z=500 m

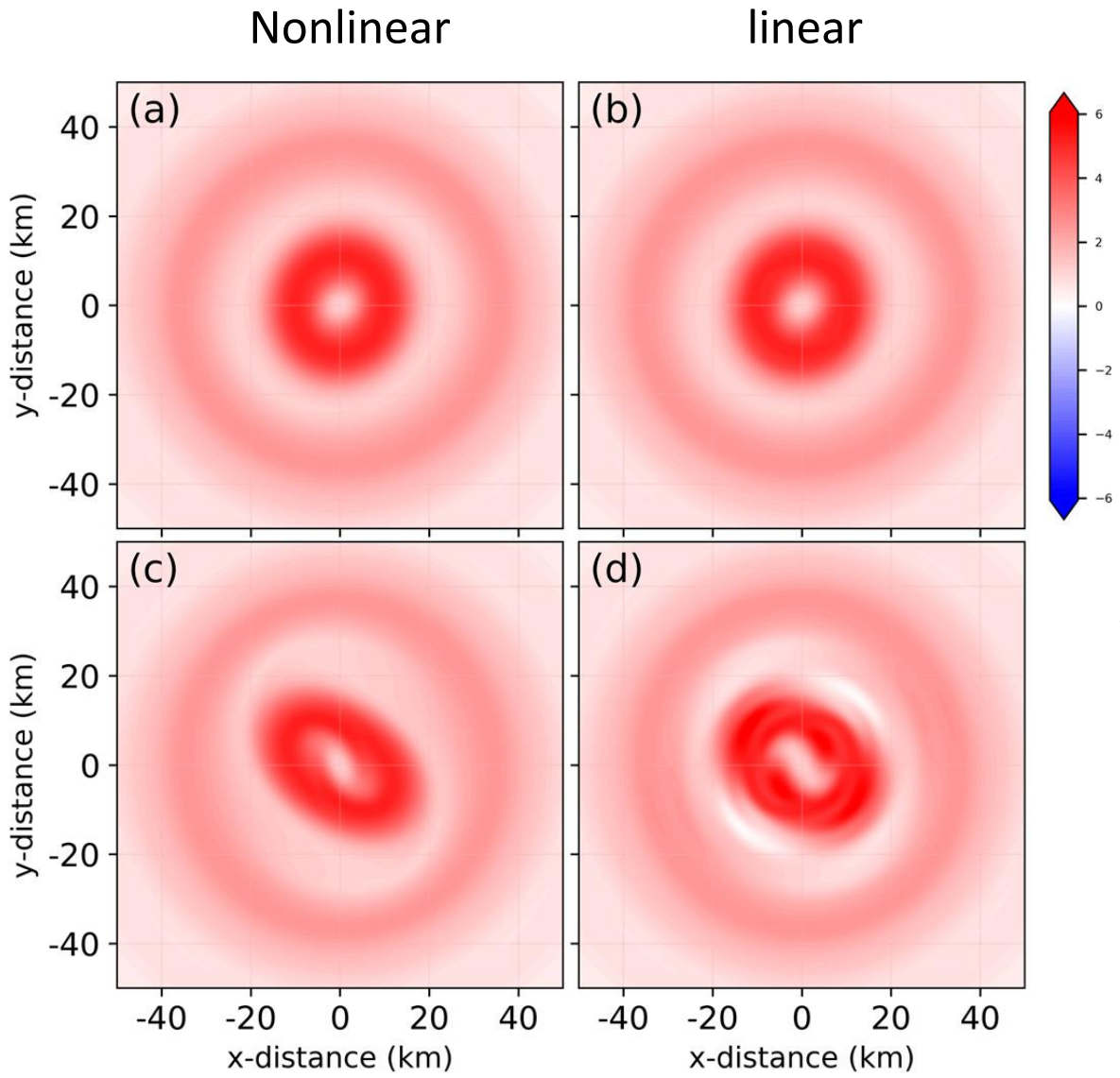

The nonlinear SWM shows a larger ellipticity, and a more well-mixed vorticity field across the moat.

Overview of the shallow water experiments

plots: azimuthally averaged AAM at inner eyewall

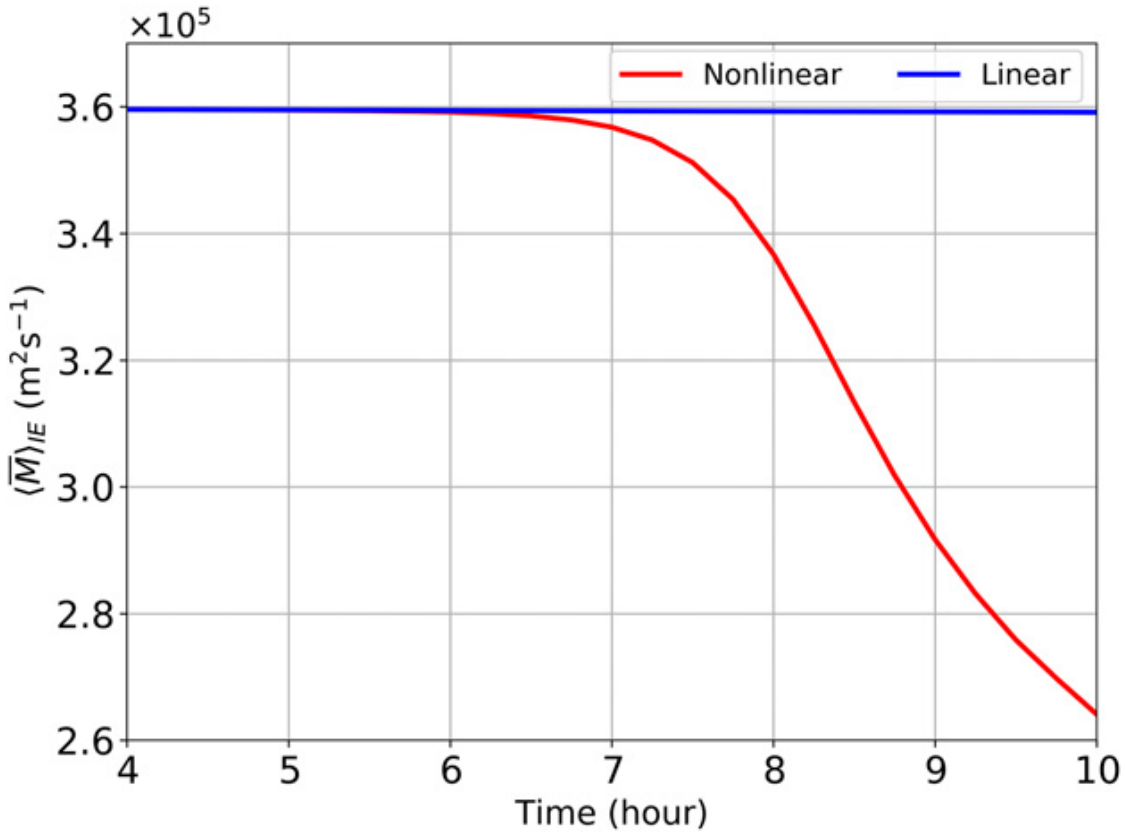

plots: azimuthally averaged AAM at outer eyewall

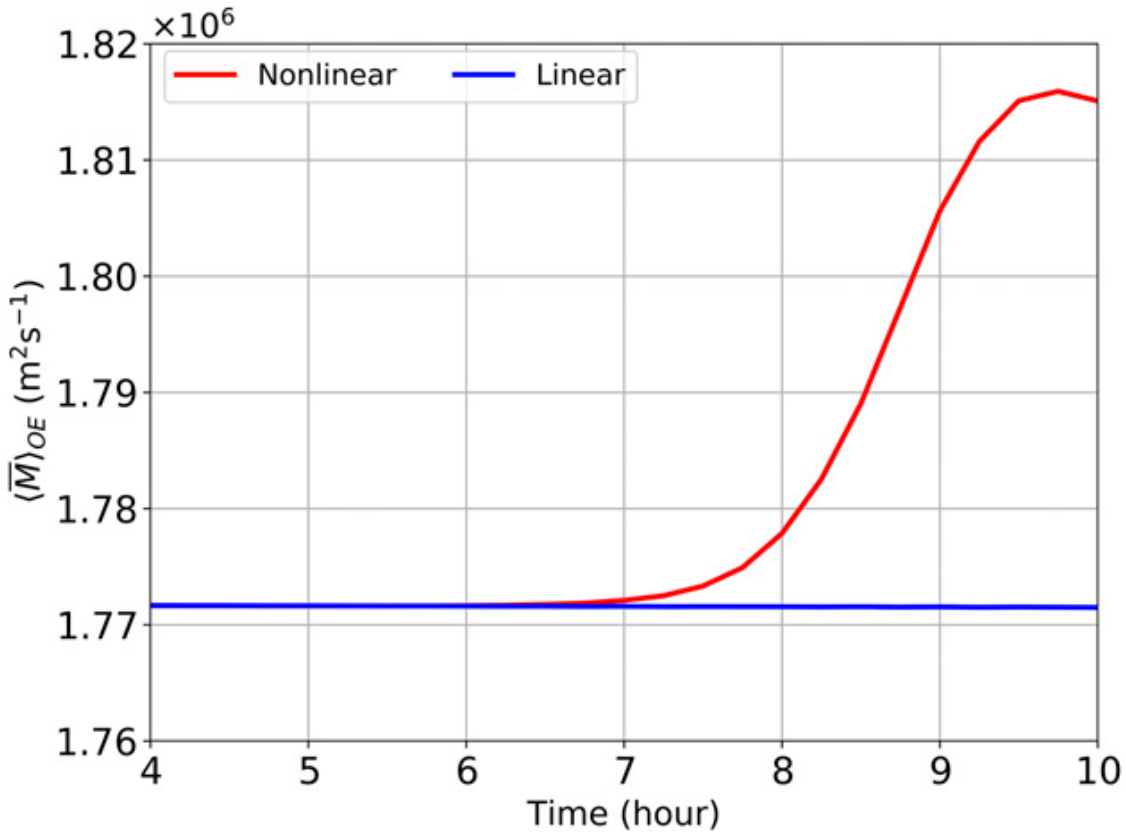

AAM budget analysis

- Convert the governing equation of SWM to cylindrical coordinates:

$$\frac{\partial V}{\partial t} + U\frac{\partial V}{\partial r} + \frac{V}{r}\frac{\partial V}{\partial \lambda} + \left(f_0 + \frac{V}{r}\right)U = -\frac{g}{r}\frac{\partial h}{\partial \lambda},$$

$\mathrm{U} = U^*$ radial wind
$\mathrm{V} = V_0 + V^*$ tangential wind
$U_0 = 0$ non-divergent

- AAM budget equation:
  - Nonlinear:

$$\frac{\partial \overline{M}}{\partial t} = -\overline{U^*}\frac{\partial \overline{M}}{\partial r} - \overline{U^{*\prime}\frac{\partial M'}{\partial r}},$$

  - Linear:

$$\frac{\partial \overline{M}}{\partial t} = -\overline{U^*}\frac{\partial \overline{M}_0}{\partial r},$$

$M = rV + \frac{1}{2}f_0 r^2$ AAM
$\bar{A}$ azimuthally averaged
A' departure from $\bar{A}$

AAM budget analysis

Inner eyewall

1 hr averaged $\overline{M}$

- LHS
- Total RHS
- Radial mean
- Radial eddy

Outer eyewall

Nonlinear

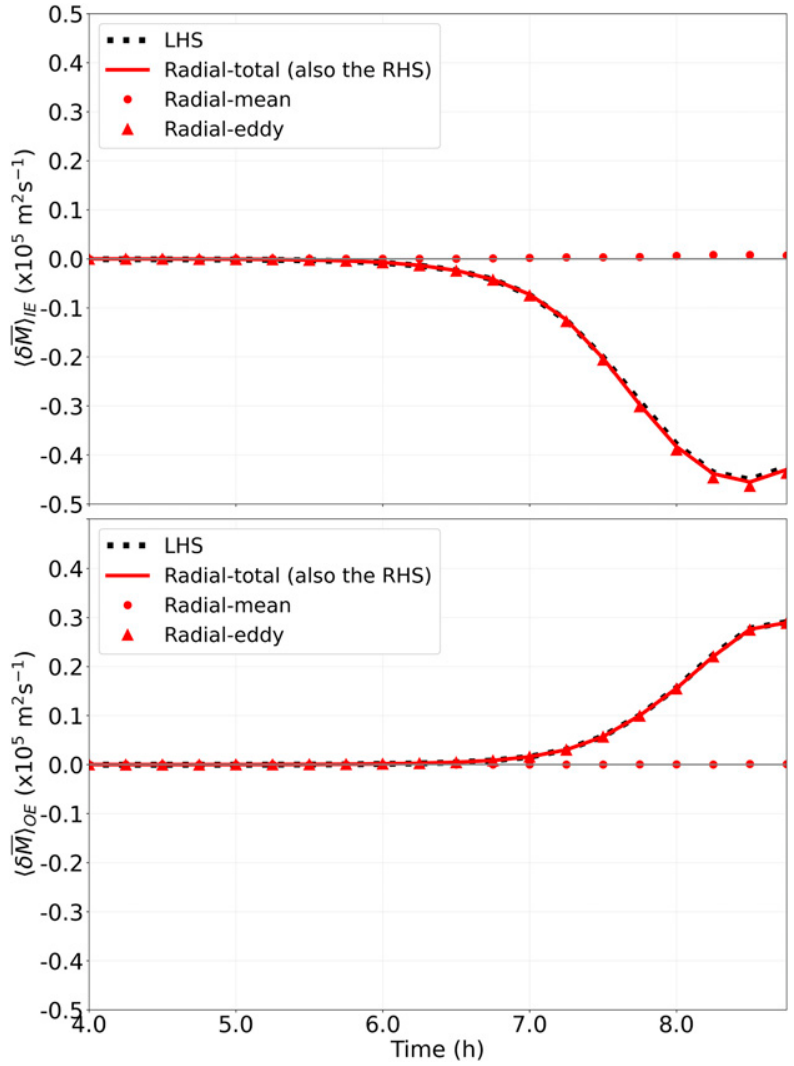

Linear

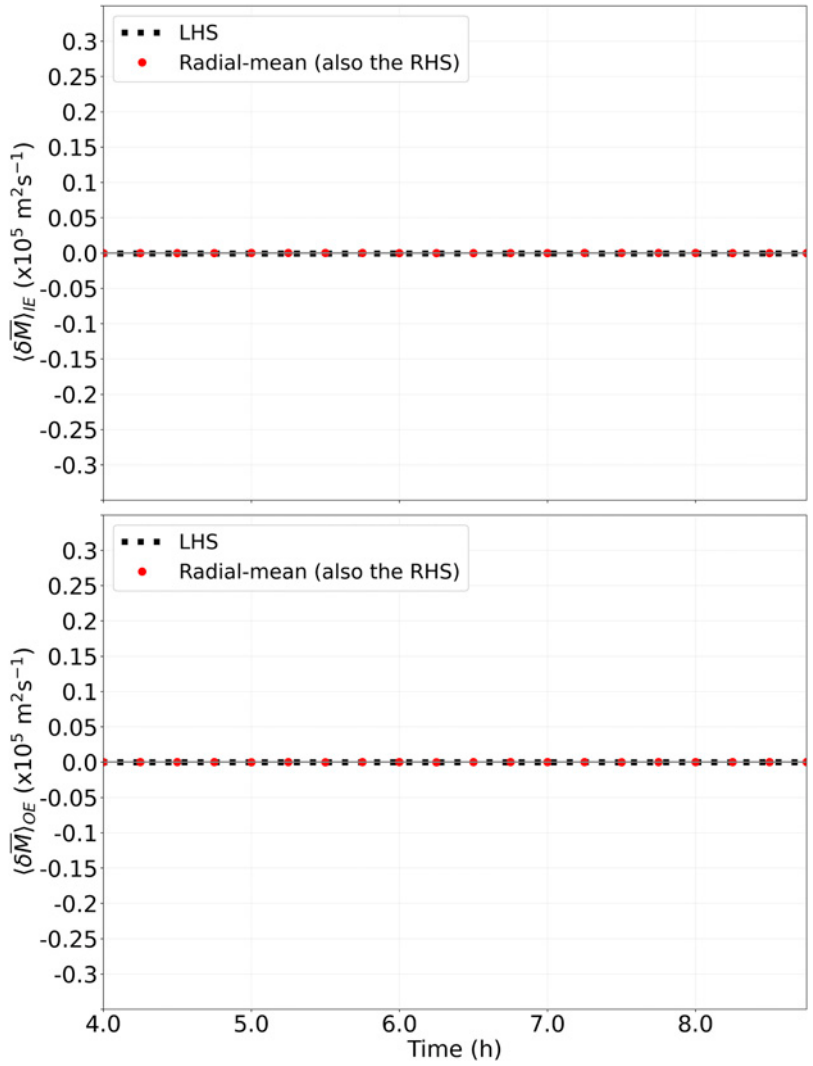

AAM budget analysis

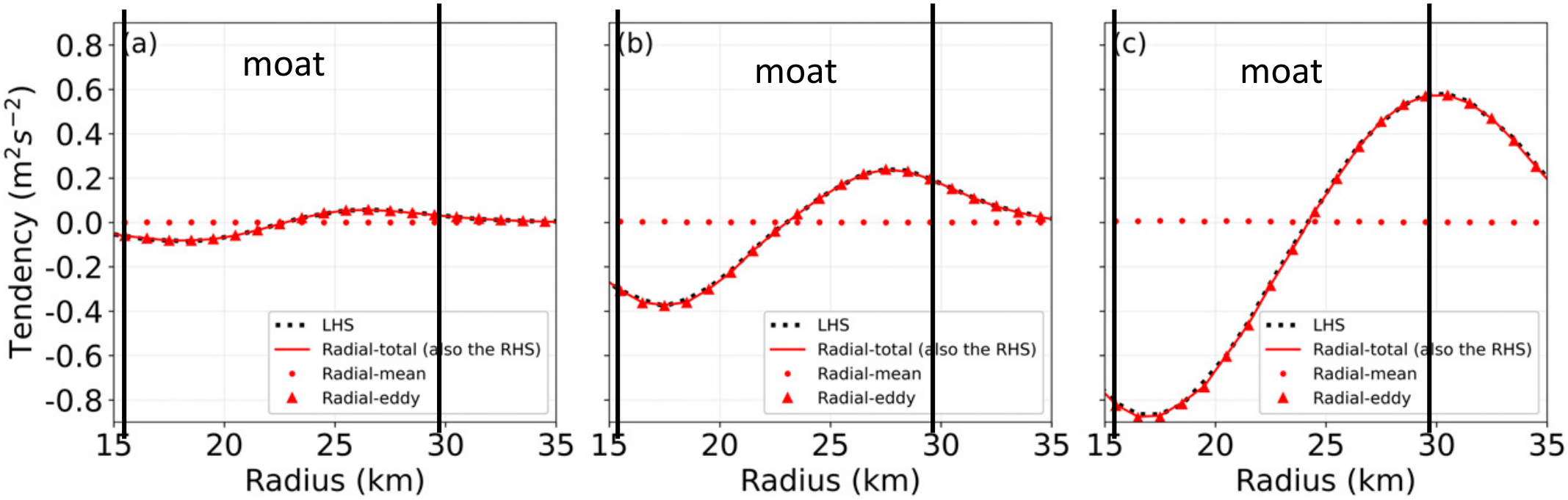

6.5 hr

7.25 hr

8.5 hr

Nonlinear 1 hr averaged $\overline{M}$

---- LHS

—— Total RHS

● Radial mean

▲ Radial eddy

Connection between the type-2 BI and the intensity changes of the eyewalls

7.5 hr at 15 km (outer part of the inner eyewall)

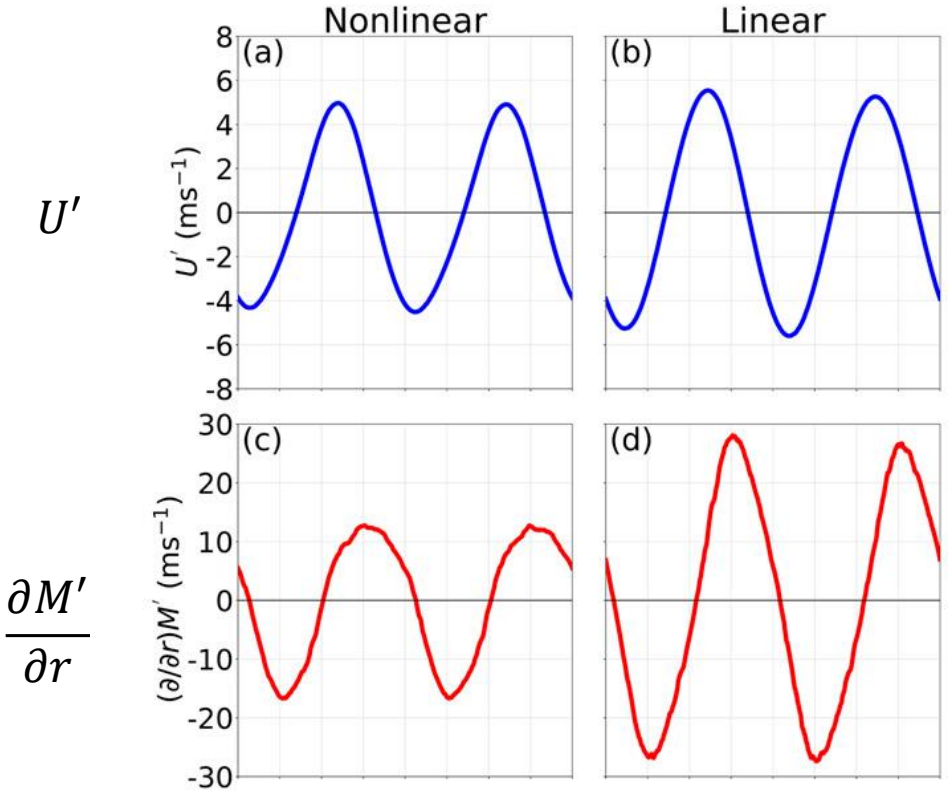

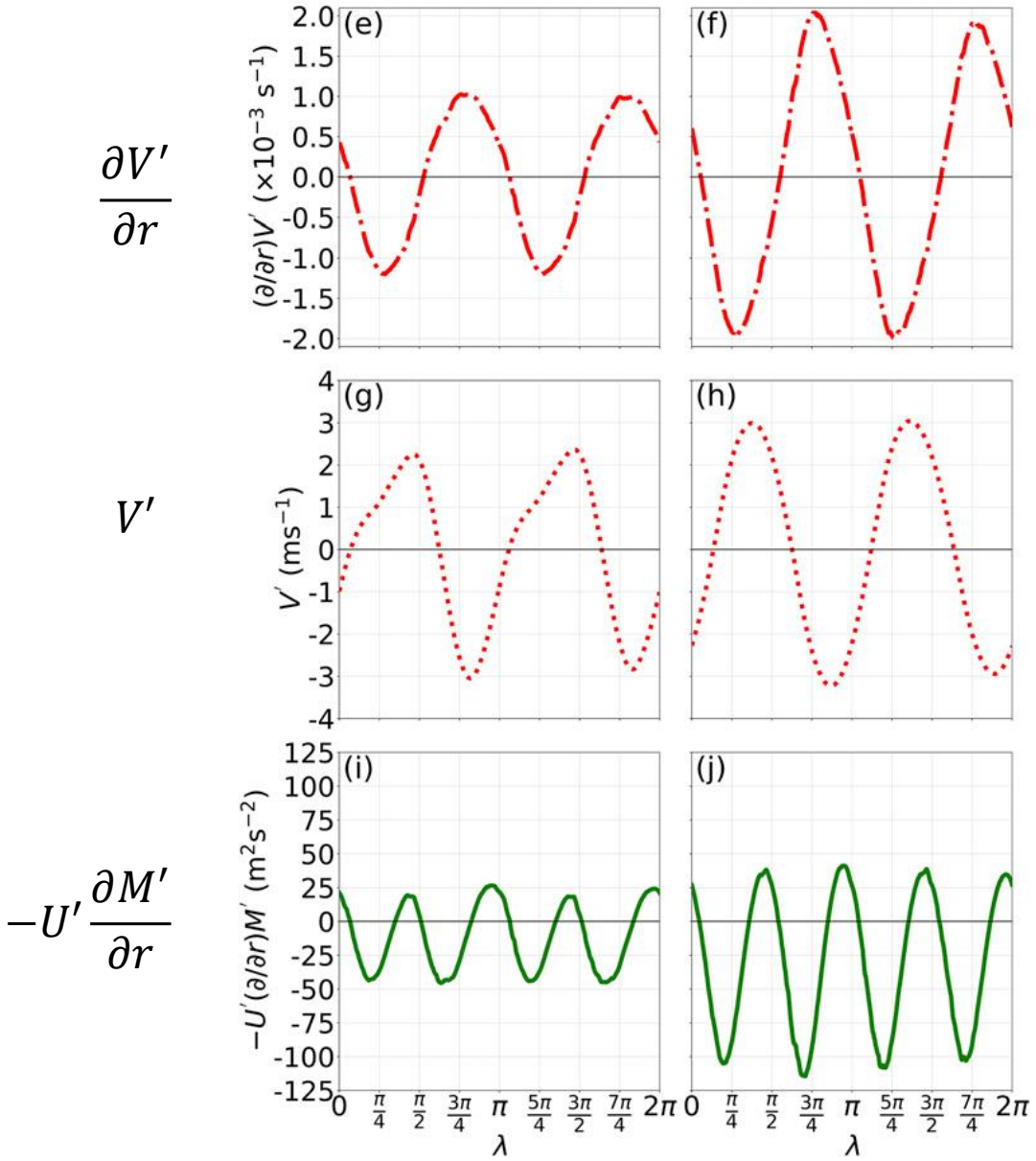

Connection between the type-2 BI and the intensity changes of the eyewalls

$$-U'\frac{\partial M'}{\partial r}$$

$$\phi_s = phase\left(\frac{\partial V'}{\partial r}\right) - phase(U')$$

If $\phi_s = 0$, $\overline{-U'\frac{\partial M'}{\partial r}} \ll 0$

If $0 < \phi_s < \frac{\pi}{4}$, $\overline{-U'\frac{\partial M'}{\partial r}} < 0$

If $\phi_s = \frac{\pi}{4}$, $\overline{-U'\frac{\partial M'}{\partial r}} = 0$

If $\frac{\pi}{4} < \phi_s < \frac{\pi}{2}$, $\overline{-U'\frac{\partial M'}{\partial r}} > 0$

If $\phi_s = \frac{\pi}{2}$, $\overline{-U'\frac{\partial M'}{\partial r}} \gg 0$

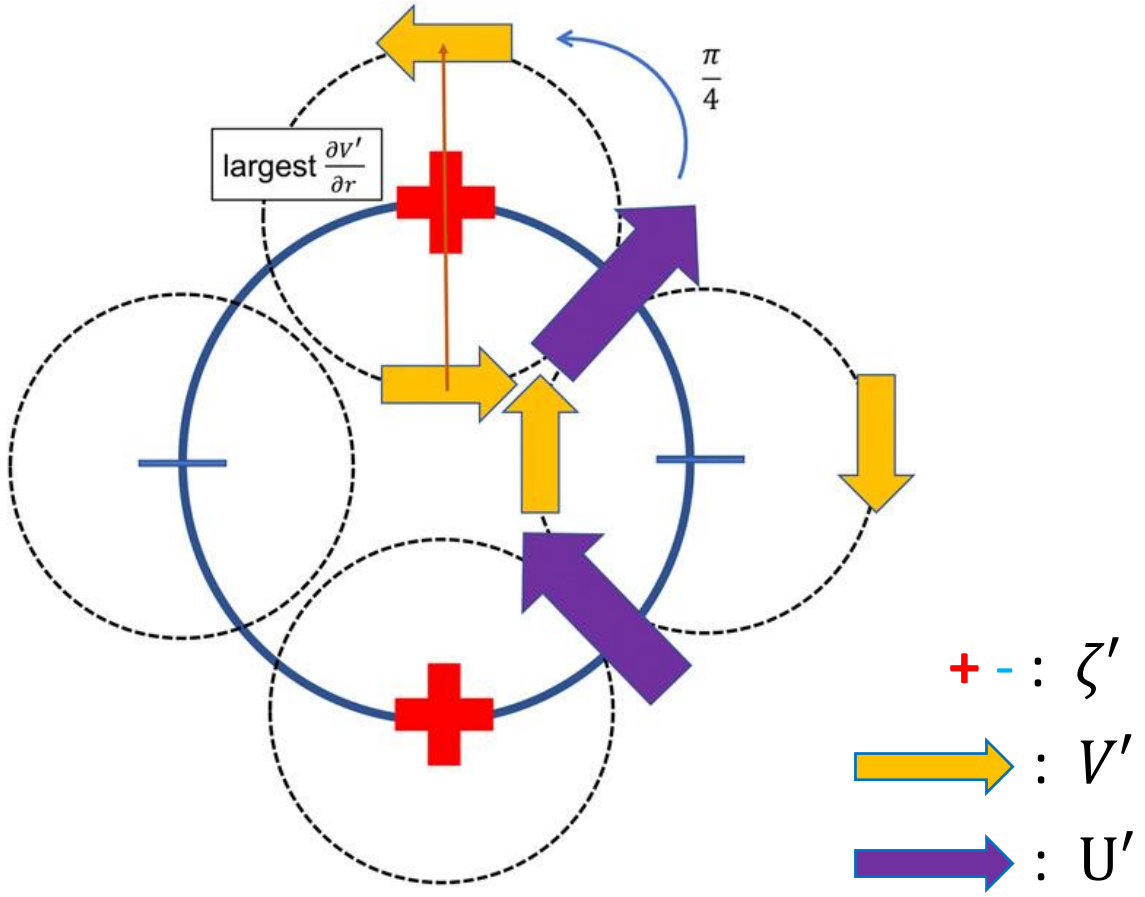

Connection between the type-2 BI and the intensity changes of the eyewalls

U'

$\frac{\partial M'}{\partial r}$

$-U'\frac{\partial M'}{\partial r}$

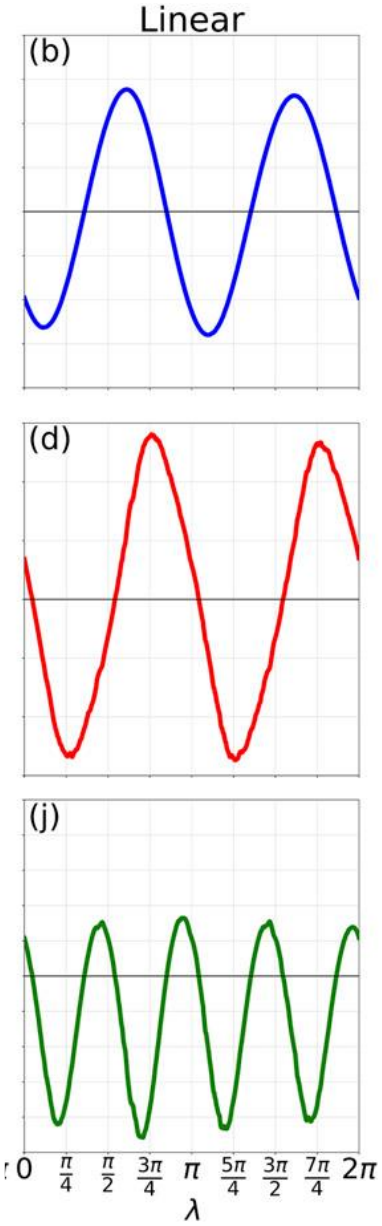

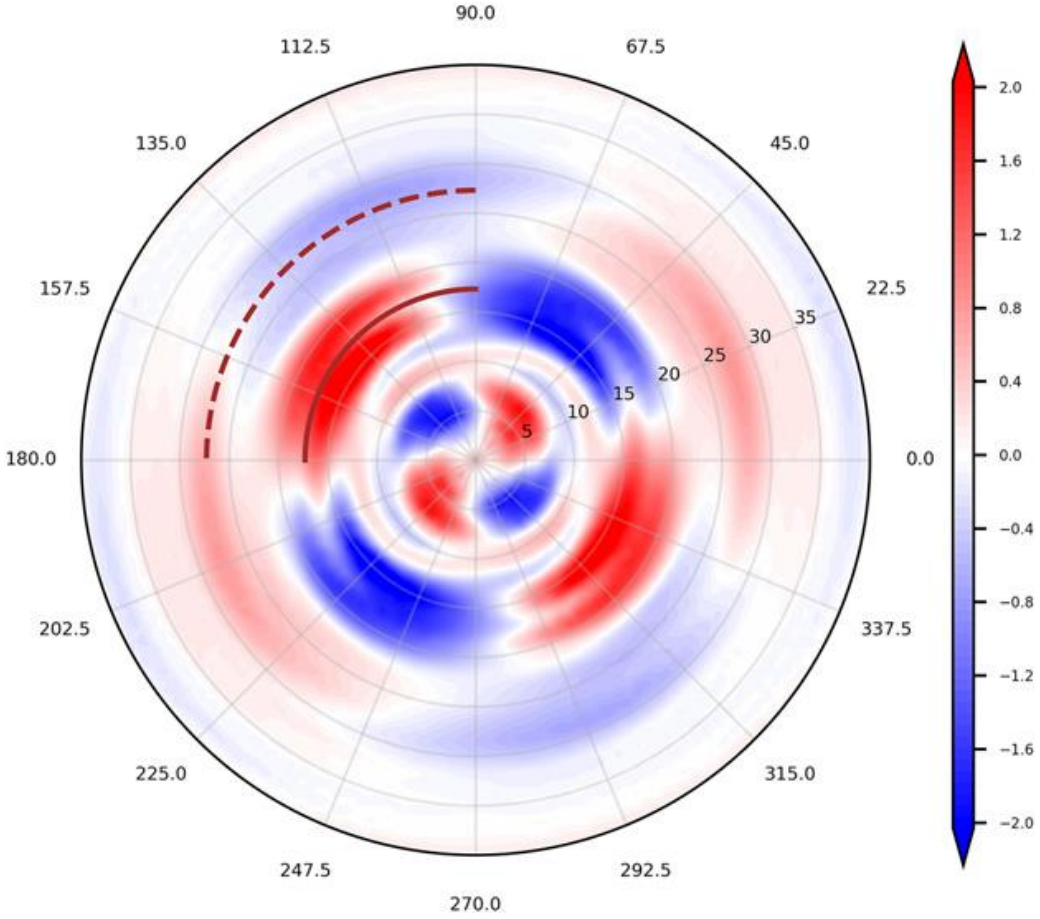

Colored: ζ'

Connection between the type-2 BI and the intensity changes of the eyewalls

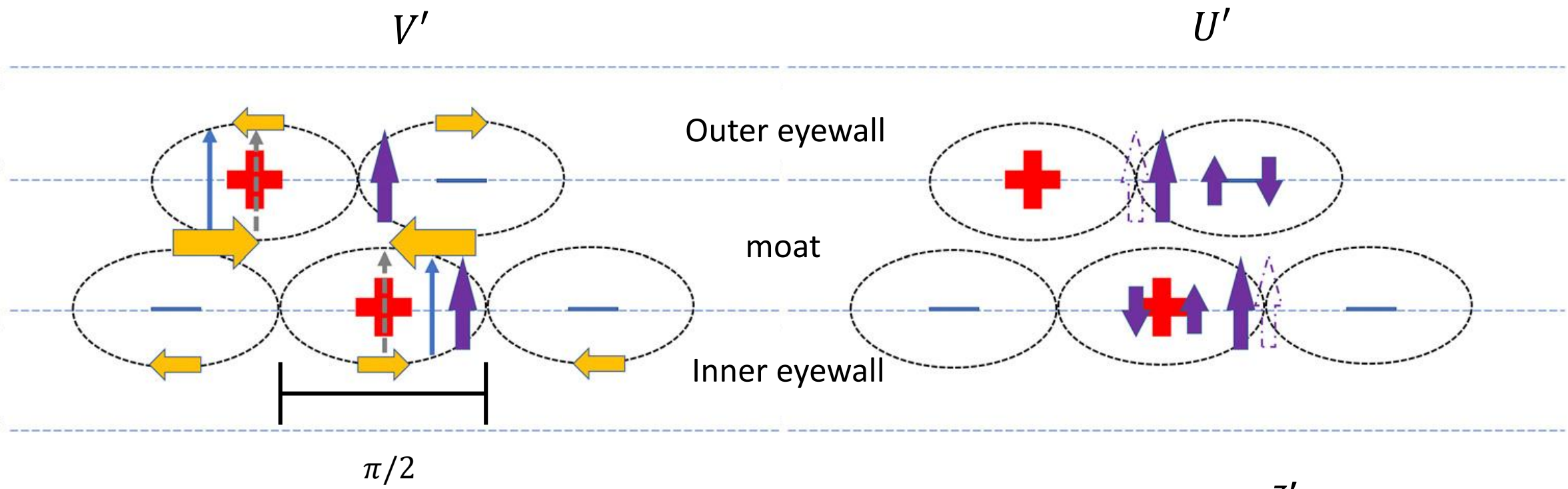

If $0 < \phi_s < \frac{\pi}{4}$, $\overline{-U' \frac{\partial M'}{\partial r}} < 0$

Connection between the type-2 BI and the intensity changes of the eyewalls

U'

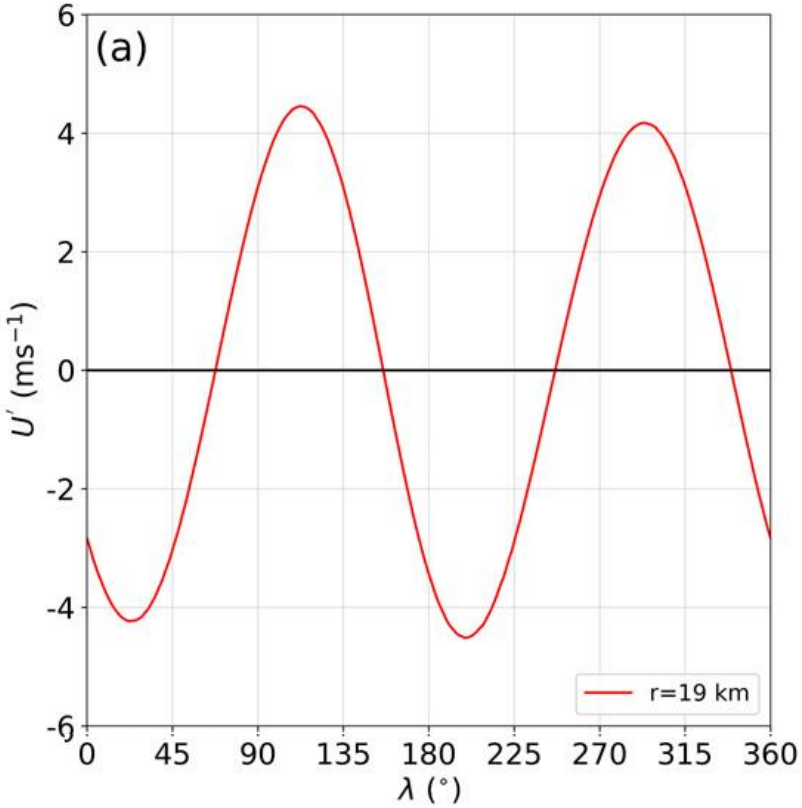

Phase change: 103.5°

V'

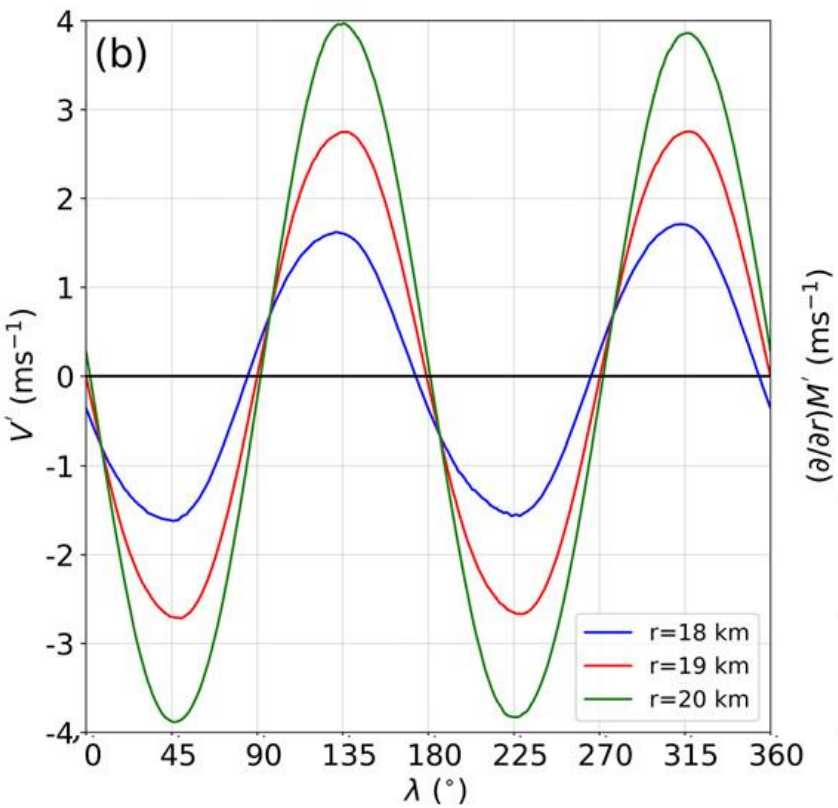

Max U': 103.5° → 110°

$\frac{\partial M'}{\partial r}$

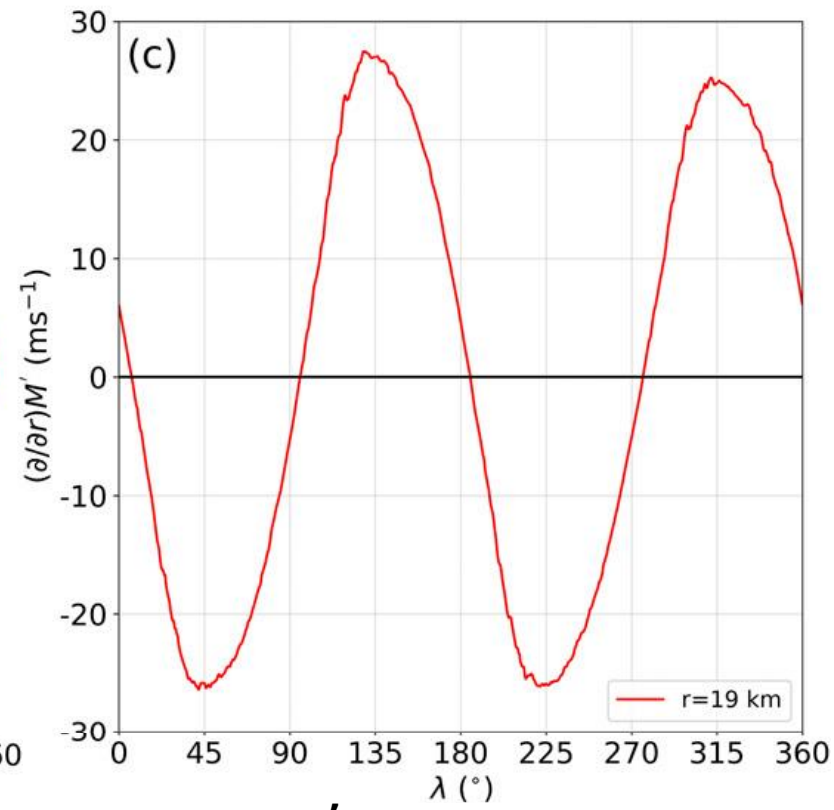

Max $\frac{\partial M'}{\partial r}$: 148.5° → 135°

ϕ_s=25°，If $0 < \phi_s < \frac{\pi}{4}$, $\overline{-U'\frac{\partial M'}{\partial r}} < 0$

Connection between the type-2 BI and the intensity changes of the eyewalls

7.5 hr at 30 km (inner part of the outer eyewall)

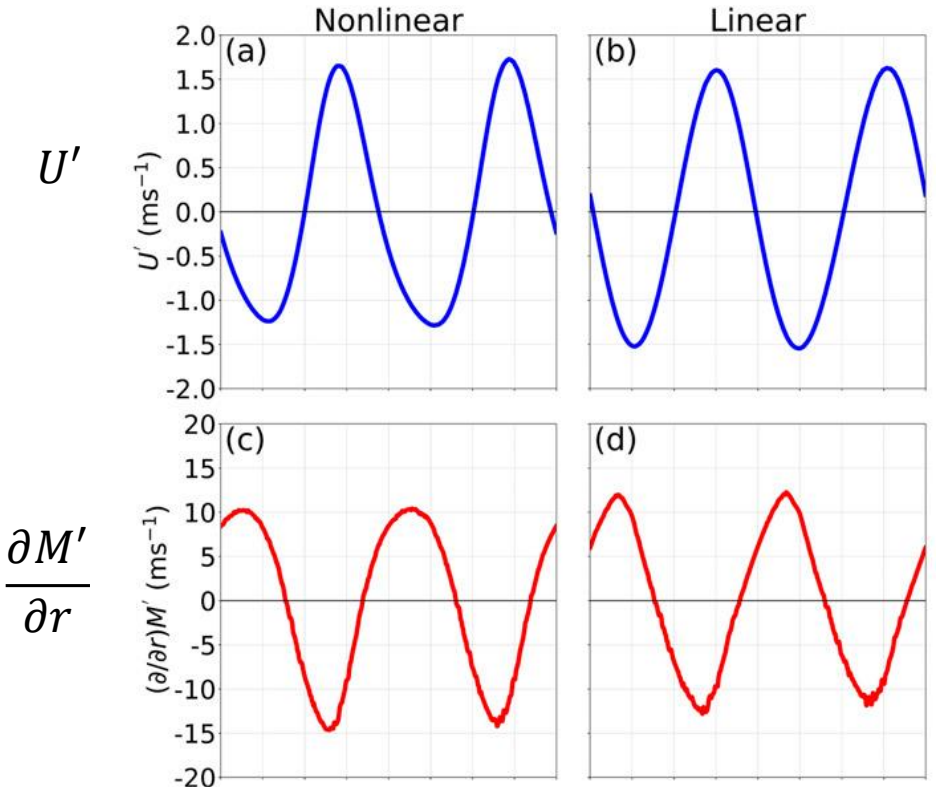

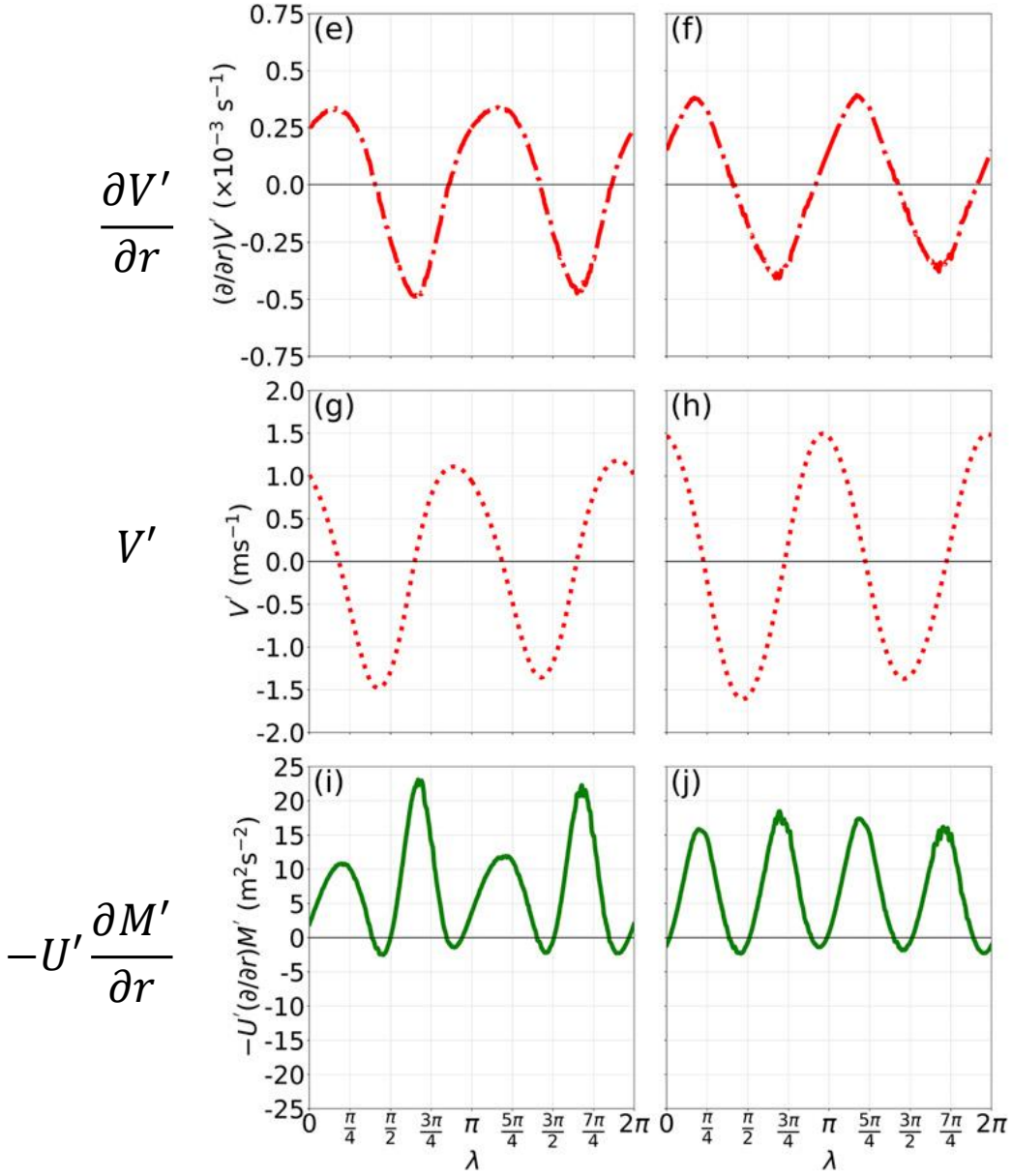

Connection between the type-2 BI and the intensity changes of the eyewalls

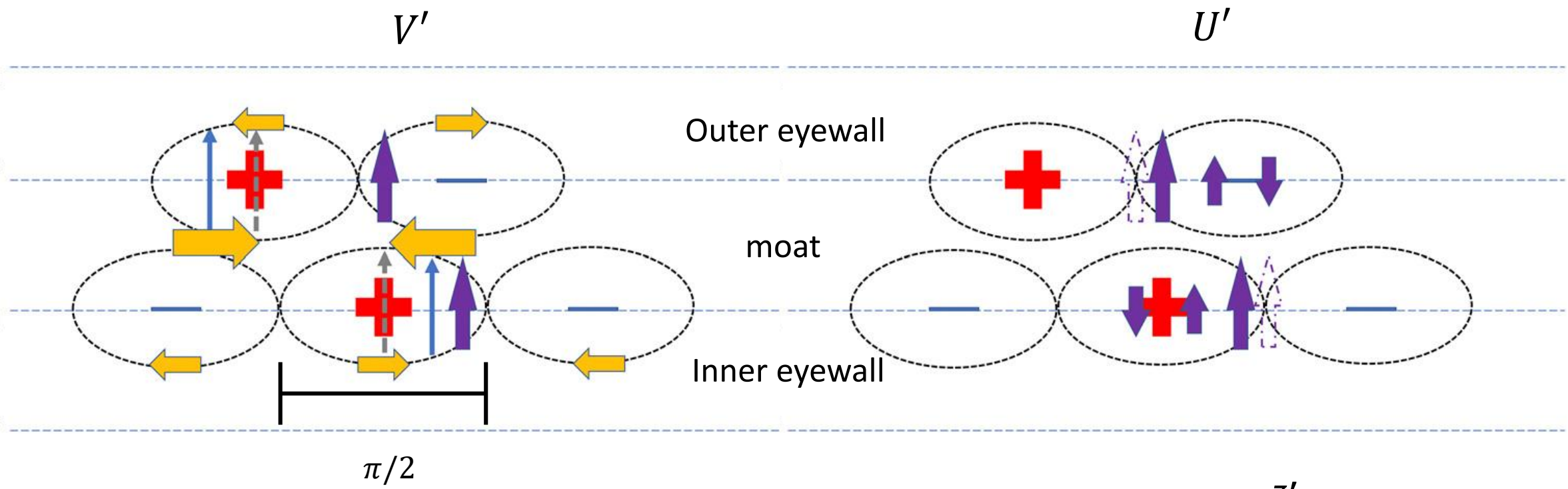

If $\frac{\pi}{4} < \phi_s < \frac{\pi}{2}$, $\overline{-U' \frac{\partial M'}{\partial r}} > 0$

Connection between the type-2 BI and the intensity changes of the eyewalls

U'

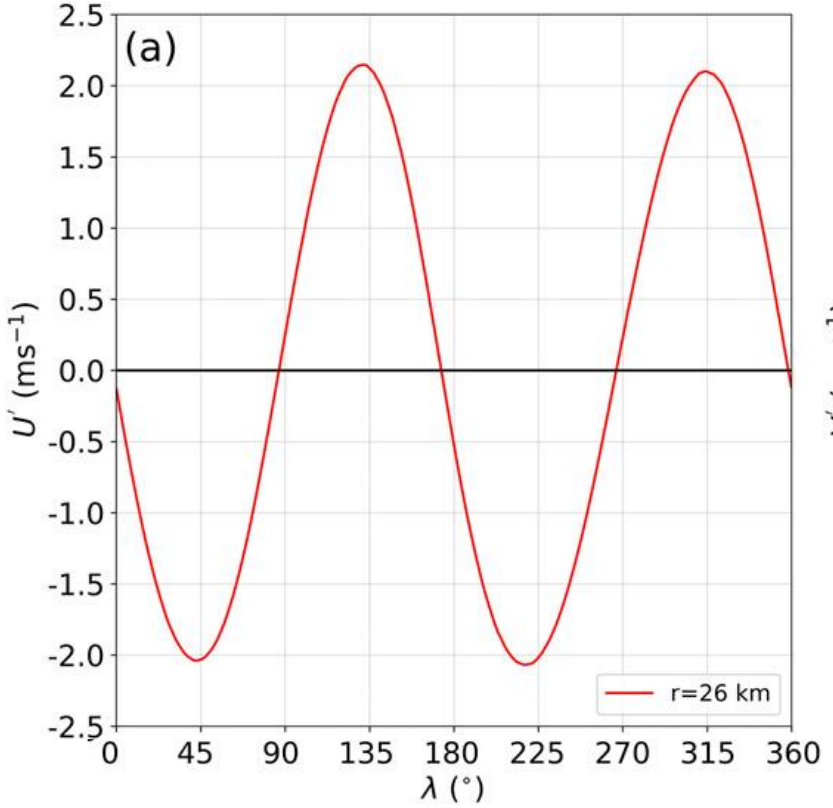

Phase change: 161°

V'

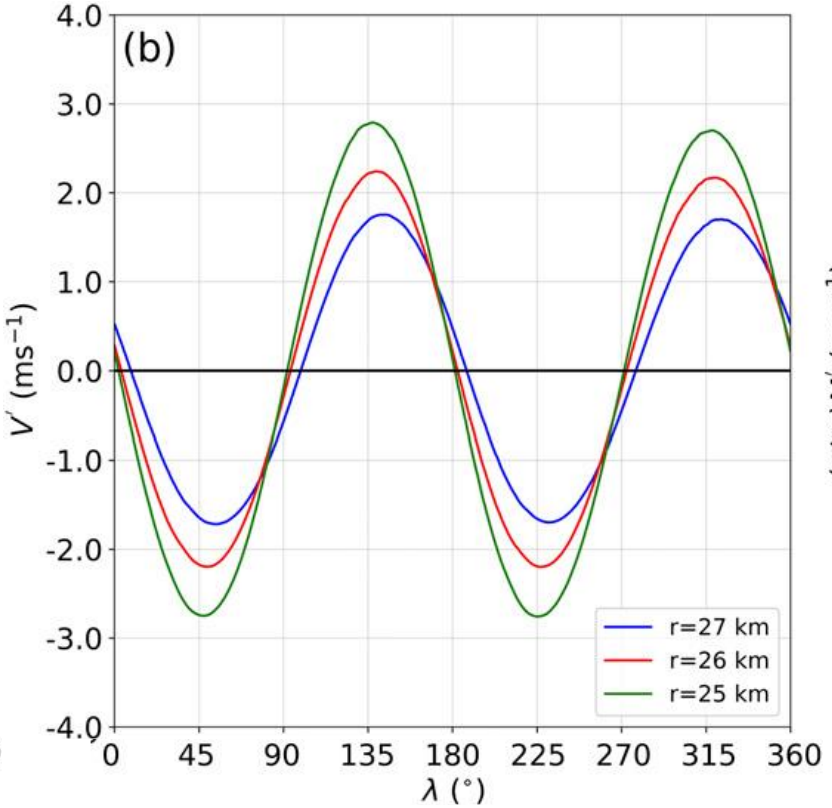

Max U': 161° → 132.2°

$\frac{\partial M'}{\partial r}$

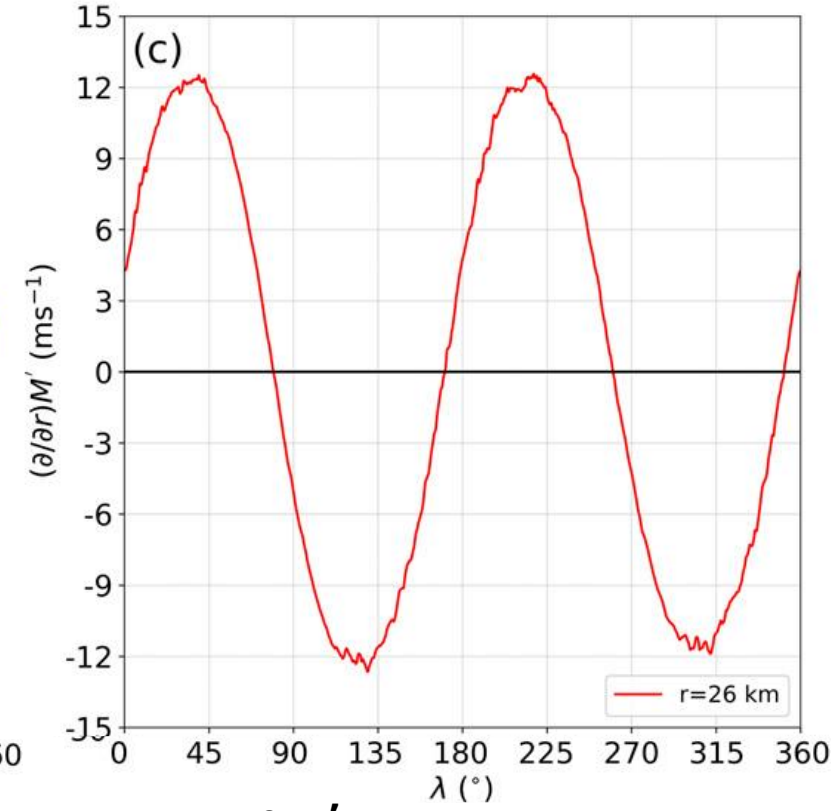

Max $\frac{\partial M'}{\partial r}$: 206° → 218.2°

ϕ_s=86°，If $\frac{\pi}{4} < \phi_s < \frac{\pi}{2}$, $\overline{-U' \frac{\partial M'}{\partial r}} > 0$

The perspective of the most unstable eigenmode on the essential dynamics

Linear stability analysis:

Linearized shallow water equations:

$$\frac{\partial u^*}{\partial t} + u_0\frac{\partial u}{\partial x} + u^*\frac{\partial u_0}{\partial x} + v_0\frac{\partial u}{\partial y} + v^*\frac{\partial u_0}{\partial y} - f_0 v = -g\frac{\partial h}{\partial x} - \nu\nabla^4 u,$$

$$\frac{\partial v^*}{\partial t} + u_0\frac{\partial v}{\partial x} + u^*\frac{\partial v_0}{\partial x} + v_0\frac{\partial v}{\partial y} + v^*\frac{\partial v_0}{\partial y} + f_0 u = -g\frac{\partial h}{\partial y} - \nu\nabla^4 v,$$

$$\frac{\partial h^*}{\partial t} + \frac{\partial(u_0 h + u^* h_0)}{\partial x} + \frac{\partial(v_0 h + v^* h_0)}{\partial y} = 0.$$

Eigenvalue problem for m:

$$\begin{bmatrix} im\frac{V_0}{r} & -\left(f_0 + \frac{2V_0}{r}\right) & g\frac{\partial}{\partial r} \\ \left(f_0 + \frac{V_0}{r} + \frac{\partial V_0}{\partial r}\right) & im\frac{V_0}{r} & im\frac{g}{r} \\ \left(\frac{H_0}{r} + H_0\frac{\partial}{\partial r}\right) & im\frac{H_0}{r} & im\frac{V_0}{r} \end{bmatrix} \begin{bmatrix} U_m \\ V_m \\ H_m \end{bmatrix} = i\omega \begin{bmatrix} U_m \\ V_m \\ H_m \end{bmatrix}$$

Turn into cylindrical coordinate and represent u^*, v^*, h^* in the Fourier expansion form:

$$A_m = \sum_{m=-\infty}^{\infty} A(r,t)e^{im\lambda}$$

The perspective of the most unstable eigenmode on the essential dynamics

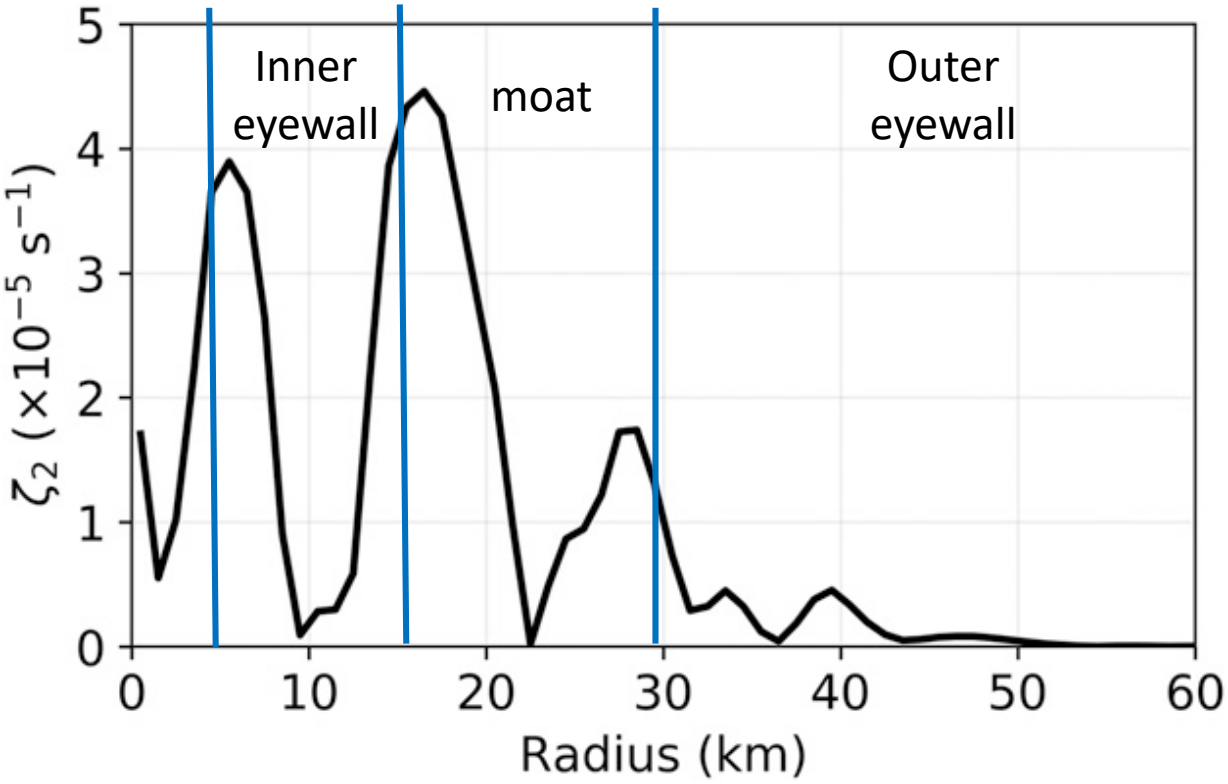

The modulus of the eigenstate ζ_2'

The most unstable mode: 2

Wave energy flux $\{U^*\phi^*\}$

$\{A\}$ azimuthally integrated

$r\{U^*V^*\}$

$\{U^*\phi^*\}$

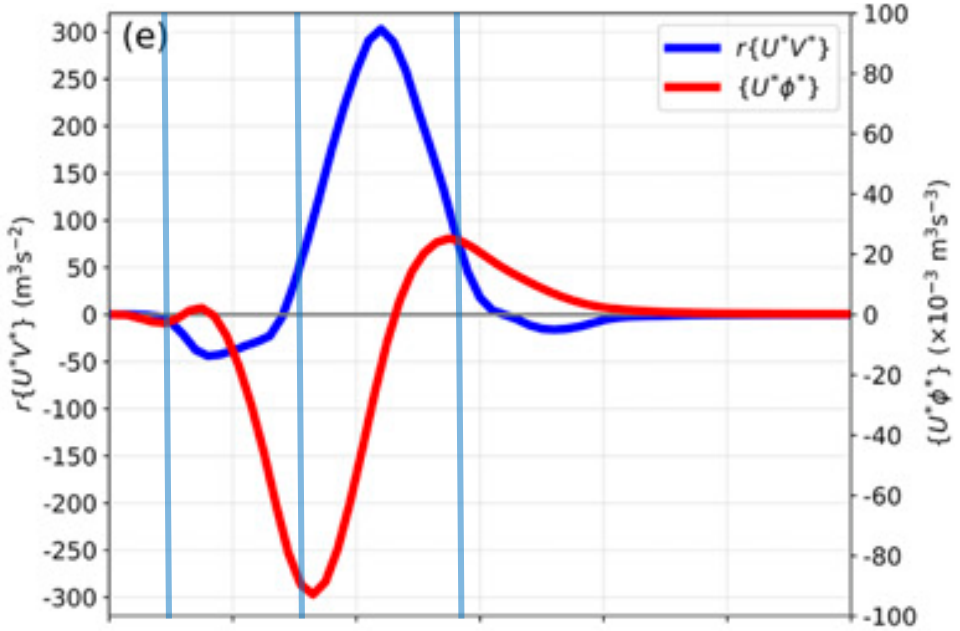

McWilliams et al. (2003)

Radial group velocity of VRW in SWM:

k: radial WN

η_0: absolute vorticity > 0

$\xi_0 = f_0 + 2V_0/r > 0$

$m = 2$

$\phi_0 > 0$

$$C_{gr} = \frac{-2mk\xi_0\left(\frac{1}{\eta_0}\frac{\partial\zeta_0}{\partial r} - \frac{1}{\phi_0}\frac{\partial\phi_0}{\partial r}\right)}{r\left[k^2 + \xi_0\left(\frac{2-\eta_0/\xi_0}{\eta_0}\right)\left(\frac{m}{r}\right)^2 + \frac{\xi_0\eta_0}{\phi_0}\right]^2},$$

$k < 0$

Eddy angular momentum flux $r\{U^*V^*\}$

Ω

Ω_{1D}

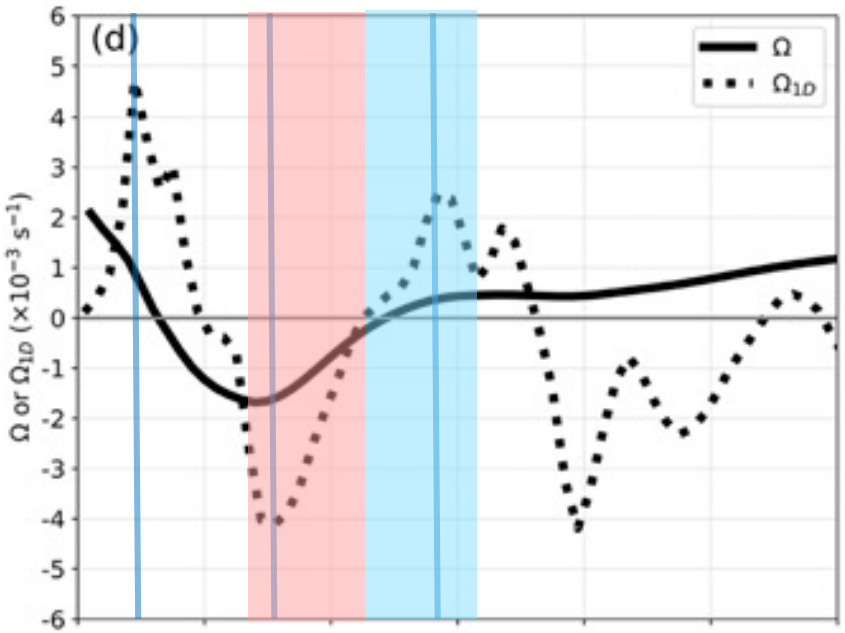

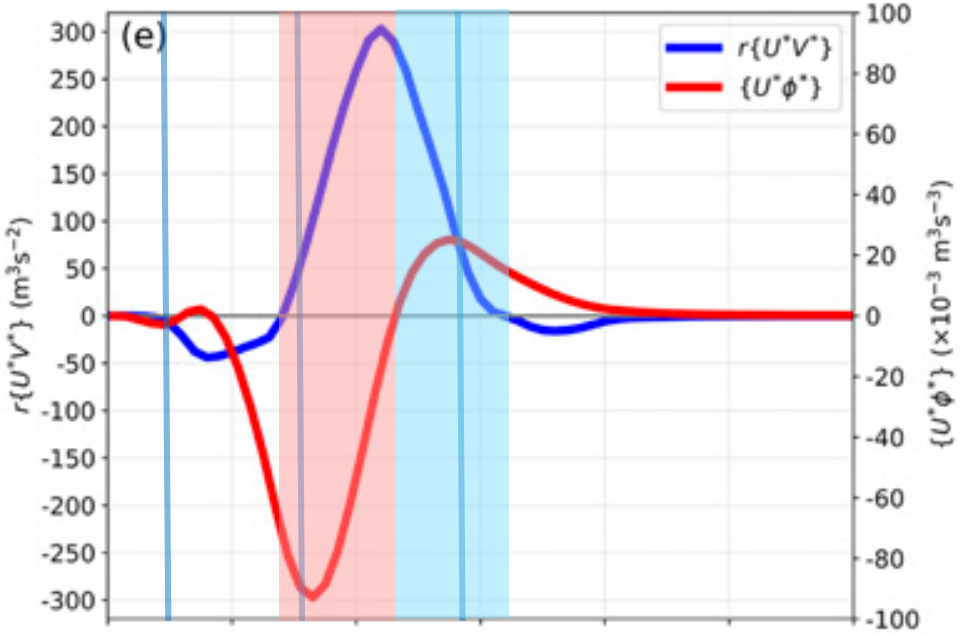

$r\{U^*V^*\}$

$\{U^*\phi^*\}$

Eliassen–Palm (E–P) relation:

Cotto et al. (2015),

$$\Omega r\{U^*V^*\} = m\{U^*\phi^*\}$$

$\Omega = \omega - mV_0/r$ Doppler-shifted angular frequency

$\Omega_{1\mathrm{D}}$ angular frequency for VRW propagation in the λ direction only

$$\Omega_{1\mathrm{D}} = \frac{\left(\frac{m}{r}\right)\left(\frac{1}{\eta_0}\frac{\partial \zeta_0}{\partial r} - \frac{1}{\phi_0}\frac{\partial \phi_0}{\partial r}\right)}{\left(\frac{2-\eta_0/\xi_0}{\eta_0}\right)\left(\frac{m}{r}\right)^2 + \frac{\eta_0}{\phi_0}}.$$

The convergence of the eddy tangential momentum flux $-r\{U^*\zeta^*\}$

$-\{U^*V^*\}$

$-r\{U^*\partial V^*/\partial r\}$

sum

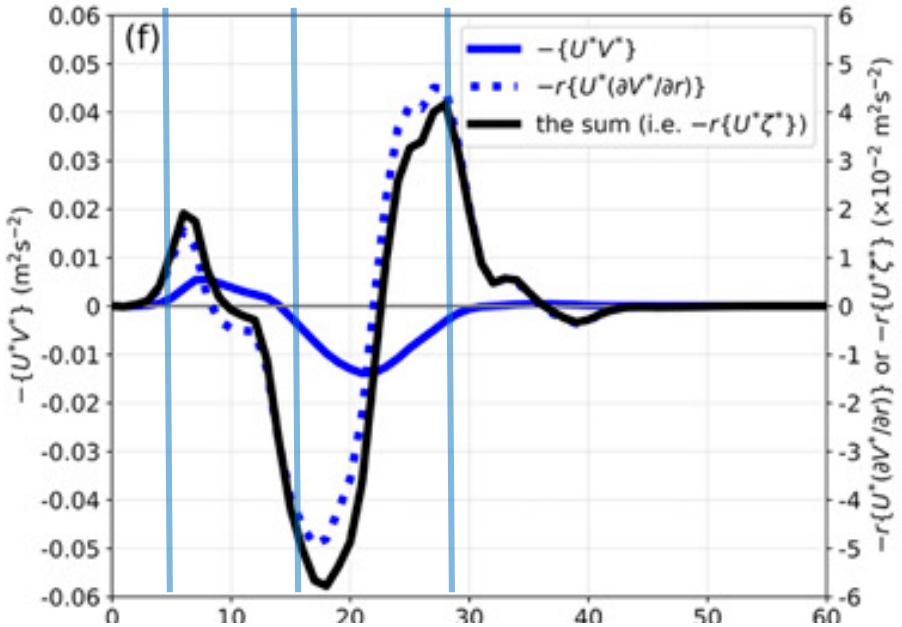

The dominating term of the AAM budget: $-r\{U^*\zeta^*\}$

Rewrite it in terms of the divergence of the eddy tangential momentum flux:

$$-r\{U^*\zeta^*\} = -r\{D(U^*V^*)\} + r\{V^*((\partial U^*)/\partial r)\}$$

$$where, D = (1/r)(\partial rF/\partial r)$$

Significance in the change in V

Threshold of RI:

$30\ kt/24\ hr$

Threshold of RW:

$-30\ kt/24\ hr$

Maximum decrease rate:

$-117\ kt/24\ hr$

Mean intensity change during weakening phase in SKR11:

$10.2\ m/s$

Nonlinear SWM

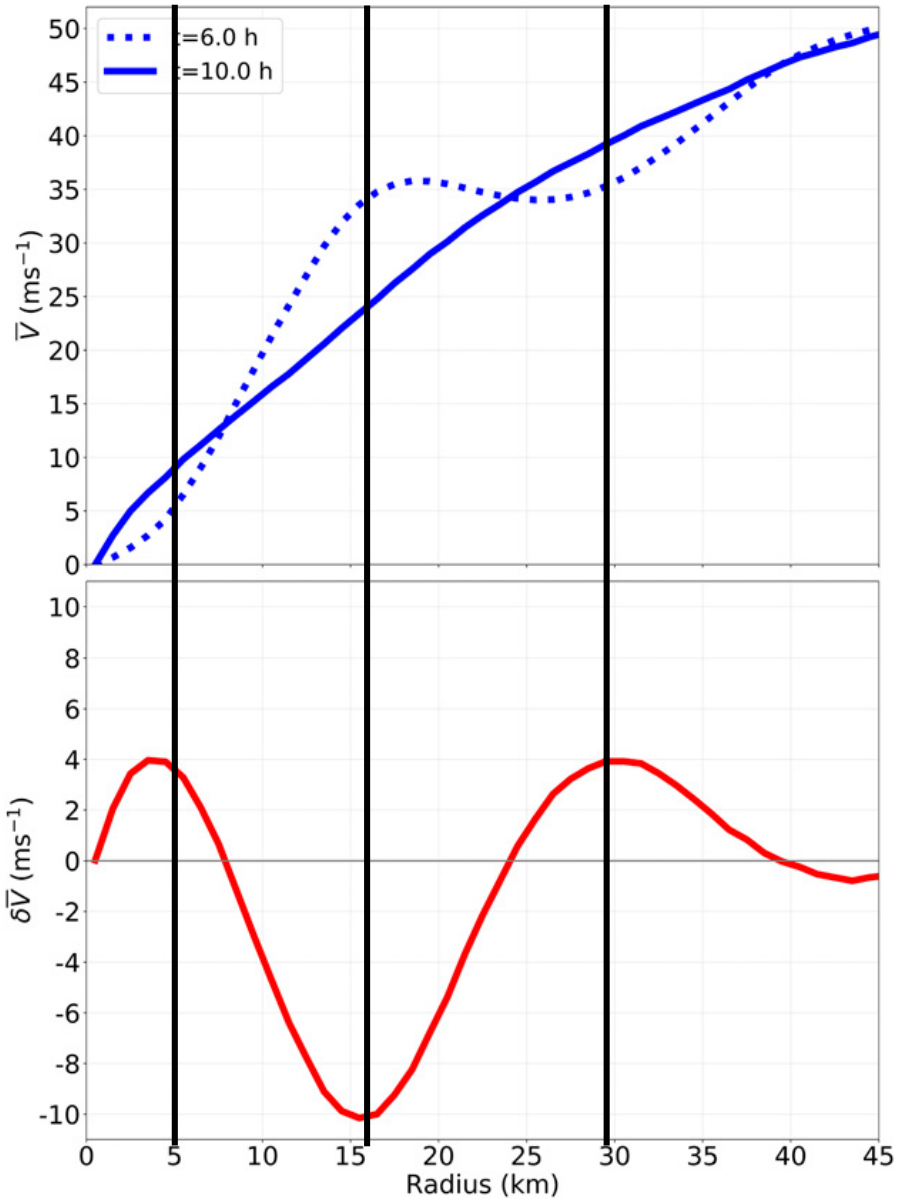

$\overline{V}$ at 6 hr

$\overline{V}$ at 10 hr

$\delta\overline{V}$

Conclusions

- The 2D SWMs show elliptical developments (WN2) of the vortices after the onset of the type-II BI. The nonlinear run shows a larger ellipticity (especially in the inner eyewall) and a more well-mixed moat than those in the linear run.

- The nonlinear run shows an increase in AAM at the outer eyewall and a decrease in AAM at the inner eyewall, while the linear run shows constant AAM at both eyewalls. The AAM change is due to the eddy radial transport of eddy AAM.

Conclusions

- The deviation of phase difference(ϕ_s) from 45° between U' and $\frac{\partial M'}{\partial r}$ is important to the decrease in inner eyewall and the increase in outer eyewall.

- The superposition of the circulation perturbation in the moat by the two VRWs change the position of the max(U') and max($\frac{\partial M'}{\partial r}$) changed. The two maximum shifted toward each other ($\phi_s < 45°$) at the inner eyewall and shifted away ($\phi_s > 45°$) at the outer eyewall.

Conclusions

- The wave energy flux $\{U^*\phi^*\}$ propagates radially inward at the outer half of the inner eyewall and the inner moat; and it propagates radially outward at the outer moat and the inner half of the outer eyewall.

- It was found that the eddy angular momentum flux $r\{U^*V^*\}$ points outward across the moat.

- The divergence and convergence of the eddy tangential momentum flux lead to the inner eyewall decay and outer eyewall intensification, respectively.

- The type-2 BI could yield an extreme weakening rate of inner eyewall $\bar{V}$, but the increase in outer eyewall $\bar{V}$ was much less significant.